Optimal Charging/Discharging Scheduling of Battery Storage Systems for Distribution Systems Interconnected With Sizeable PV Generation Systems

Jen-Hao Teng, *Senior Member, IEEE*, Shang-Wen Luan, Dong-Jing Lee, and Yong-Qing Huang

***Abstract*—Utilizing battery storage systems (BSSs) can reduce the intermittent output of PV generation systems (PVGSs) and make them dispatchable. The aim of this paper is to design an optimal charging/discharging scheduling for BSSs such that the line loss of distribution systems interconnected with sizeable PVGSs can be minimized. A mathematical model for BSSs which can be used to simulate the charging procedures such as the commonly-used constant current to constant voltage (CC-CV) charging method, the discharging procedures and the state of charge (SOC) is proposed first. The minimum line loss problem considering the intermittent output of PVGSs and the scheduling of BSSs is then formulated based on the BSS mathematical model. The optimal charging/discharging scheduling of BSSs can then be obtained by a genetic algorithm (GA) based method. Test results demonstrate the validity of the proposed mathematical model and optimal charging/discharging scheduling for BSSs.**

***Index Terms*—Battery storage system, charging/discharging scheduling, genetic algorithm, photovoltaic generation system, state of charge.**

I. Introduction

RENEWABLE energy generation systems (REGSs), such as photovoltaic (PV), wind, biomass, etc., have increasingly important roles as power supplies due to the needs to reduce pollutant gas emission and the liberalization of electrical market. In particular, PV and wind are expected to become a larger part of energy portfolio during the next couple of decades [1]. Many interconnection requirements and regulations for REGSs have been developed. However, even if a REGS has passed all of the requirements of interconnection regulation, the online operation of REGSs may raise some unpredictable problems for power grids due to the intermittent output characteristic of REGSs. Serious operating problems might occur when high percentages of renewable generations are integrated into power grids. Consequently, some papers recommended that the outputs of REGSs should be constrained [2], [3]. To mitigate the impacts of the interconnection of REGSs, the concepts of smart grid are proposed widely [4]–[8]. Although smart grid can effectively monitor REGSs, it cannot directly manage and control intermittent output characteristic of REGSs. Therefore, one of the major challenges for REGSs remains in matching the intermittent energy production with the dynamic power demand. A recommended solution is to add battery storage systems (BSSs) to these intermittent REGS. The hybrid system composed of REGSs, local loads, BSSs, and the grid can be used to reduce the impacts of REGSs [9]–[19].

The dispatch of hybrid system is a cumbersome task due to the complications and varieties of the hybrid system. Many papers have aimed to solve the operating scheduling for the hybrid system. [16] proposed a determinist energy management system for a micro-grid, including advanced PV generators with embedded storage units and a gas micro-turbine. [17] analyzed the impact of grid-connected PV/battery system on locational pricing, peak load shaving, and transmission congestion management. [18] proposed a rule-based control of battery energy storage for dispatching intermittent renewable sources and discussed the effectiveness of control strategies. [19] proposed an optimal power management mechanism for grid connected PV generation system (PVGS) with storage and optimization achieved by dynamic programming. Although these papers focused on the operation of hybrid system, a practical and realistic mathematical model for BSS which can be used to simulate the charging procedure using, for example, the commonly-used constant current to constant voltage (CC-CV) charging method, the discharging procedure and the state of charge (SOC) still needs to be investigated. The mathematical model should also be applicable for power system analysis under different operating conditions. Therefore, this paper aims to design a mathematical model of BSS and use this model for power system analysis.

Traditionally, the BSSs are charged and discharged in off-peak load and peak load hours, respectively. However, to cope with the intermittent output of PVGSs, the charging/discharging scheduling of BSSs should be arranged at least hourly with respect to the load variations and intermittent outputs of PVGSs. If the interactions between loads, PVGSs and BSSs can be determined effectively, advantages of BSSs such as line loss reduction, power quality enhancement, and reliability improvement, interconnection impact reduction of REGS, can be achieved. The minimum line loss problem considering the intermittent

Manuscript received March 12, 2012; revised May 26, 2012; accepted November 19, 2012. Date of publication December 11, 2012; date of current version April 18, 2013. This work was supported in part by Industrial Technology Research Institute and National Science Council under Grand NSC 100-2221-E-110-090-MY3 and NSC 100-3113-p-110-004. Paper no. TPWRS-00192-2012.

J.-H. Teng is with the Department of Electrical Engineering, National Sun Yat-Sen University, Kaohsiung, Taiwan (e-mail: jhteng@ee.nsysu.edu.tw).

S.-W. Luan is with the Department of Electrical Engineering, I-Shou University, Kaohsiung, Taiwan (e-mail: sunwin56@gmail.com).

D.-J. Lee and Y.-Q. Huang are with the Green Energy and Environment Research Laboratories, Industrial Technology Research Institute, Hsinchu, Taiwan (e-mail: leedongjing@itri.org.tw; itri960611@itri.org.tw).

Color versions of one or more of the figures in this paper are available online at http://ieeexplore.ieee.org.

Digital Object Identifier 10.1109/TPWRS.2012.2230276

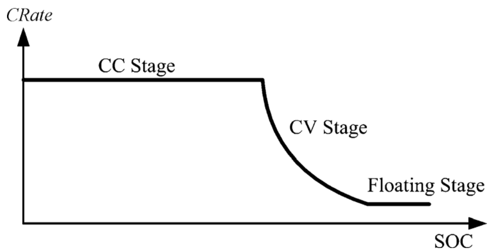

Fig. 1. CC-CV charging scheduling.

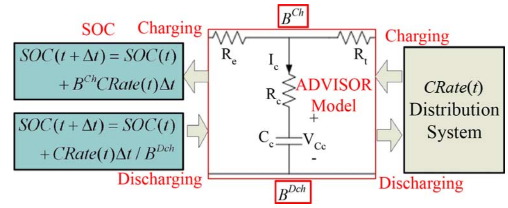

Fig. 2. SOC estimation considering the heating effect caused by the electrochemistry reaction.

outputs of PVGSs, load variations and the scheduling of BSSs is formulated in this paper. The optimal charging/discharging scheduling of BSSs can then be solved by a genetic algorithm (GA) based method. Test results demonstrate the validity of the proposed method.

II. Mathematical Model for BSS

Conventional battery charging method occurs in two stages: the battery is charged at a constant current until the battery voltage reaches the predefined upper voltage limit (CC stage), followed by a constant voltage charging until the current reaches a predetermined small value (CV stage). Sometimes, a small charging current will charge the battery and be treated as a floating stage. This method is often called CC-CV charging method and its charging scheduling is illustrated in Fig. 1. There are some mathematical models used to simulate the transient behaviors of batteries during the charging/discharging procedure [20]–[24]; however, they are often too complicated and time-consuming, since these models used differential equations to estimate the battery status. Therefore, these battery models cannot be used in steady-state power system analysis efficiently. In addition, the SOC in the whole charging/discharging procedure must be estimated as well. Although, many SOC estimation algorithms have been proposed [24]–[27]; the terminal voltage method and coulometric measurement method are the simplest and most practical algorithms to effectively estimate the SOC variation of BSS. For a charging or discharging current at the time t, $CRate(t)$, the SOC variation estimated by the coulometric measurement method [25]–[27] can be written as

$$SOC(t+\Delta t) = SOC(t) + CRate(t)\Delta t \tag{1}$$

where $SOC(t+\Delta t)$ and $SOC(t)$ are the SOC at the time $t+\Delta t$ and t, respectively. Positive and negative $CRate(t)$ indicate charging and discharging, respectively.

Note that the commonly used unit for charging/discharging currents in (1) is the rated capacity (denoted as C) of a BSS and the charging/discharging currents are expressed as percentages of C. Although (1) provides a simple way to estimate the SOC during charging/discharging procedure, the heating effect caused by the electrochemistry reaction of battery, which may degrade SOC, cannot be considered in the coulometric measurement method. ADVISOR battery model as proposed in [21]–[23] uses the combination of capacitors and resistors to model the electrochemistry reaction of battery. ADVISOR model can be used to estimate the SOC variation. However, it is time-consuming and too complicated to be used in power system analysis. Therefore, a compromising scheme is proposed in this paper. The SOC degradation due to the heating effects caused by the electrochemistry reaction in the charging and discharging procedures are modeled by two efficiency parameters B^{Ch} and B^{Dch}, respectively. For example, if B^{Ch} is 97%, it means that 3% SOC, that is $1-B^{Ch}$, is degraded due to the heat caused by the electrochemistry reaction. B^{Ch} and B^{Dch} depend on the used battery types, charging/discharging currents, life time cycle and state of health of the BSSs [20]–[24]. Fig. 2 illustrates the compromising scheme proposed in this paper. From Fig. 2, it can be seen that B^{Ch} and B^{Dch} are used to replace the heating effects on the SOC degradation and the SOC in the charging/discharging procedures can be expressed as

$$\begin{aligned}&if\ CRate(t) \geq 0\ then\\ &SOC(t+\Delta t) = SOC(t) + B^{Ch}CRate(t)\Delta t \qquad \text{(2a)}\\ &if\ CRate(t) \geq 0\ then\\ &SOC(t+\Delta t) = SOC(t) + B^{Ch}CRate(t)\Delta t. \qquad \text{(2b)}\end{aligned}$$

For the CC stage, the charging current stays constant ($CRate_{CC}^{ch}$ as shown in Fig. 3) and the SOC variation can be estimated by (2). The charging current in the CV stage as shown in Fig. 1 will decrease gradually. The charging current cannot be easily estimated; as a result, the SOC in the CV stage cannot be effectively estimated neither. However, researches have revealed that the SOC can be roughly approximated by the terminal voltage of battery [25]–[27]. Therefore, when the SOC in the CC stage reaches a predefined upper value (SOC_{CC}^{Ch}), which means that battery voltage roughly reaches the predefined upper voltage limit, the CC stage will be changed to the CV stage accordingly. Similarly, when the SOC in the CV stage reaches a predefined upper value (SOC_{CV}^{Ch}), the CV stage will be changed to the floating stage. A piecewise CC charging process as shown in Fig. 3 is used in the CV stage in this paper. Fig. 3 illustrates that the CV stage is divided into several sub-stages and each sub-stage can be regarded as a CC charging. Using three sub-stages as an example, the mathematical model of CV stage can be expressed as

$$\begin{aligned}&if\ SOC_{CC}^{Ch} < SOC(t) \leq SOC_{CV,1}^{Ch}\\ &CRate(t) = CRate_{CV,1}^{Ch}\\ &else\ if\ SOC_{CV,1}^{Ch} < SOC(t) \leq SOC_{CV,2}^{Ch}\\ &CRate(t) = CRate_{CV,2}^{Ch}\\ &else\ if\ SOC_{CV,2}^{Ch} < SOC(t) \leq SOC_{CV,3}^{Ch}\\ &CRate(t) = CRate_{CV,3}^{Ch}\end{aligned} \tag{3}$$

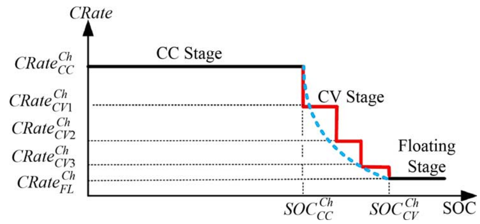

Fig. 3. Proposed piecewise CC charging for CV stage.

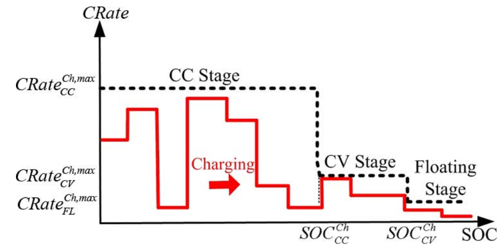

Fig. 4. Charging scheduling for BSSs.

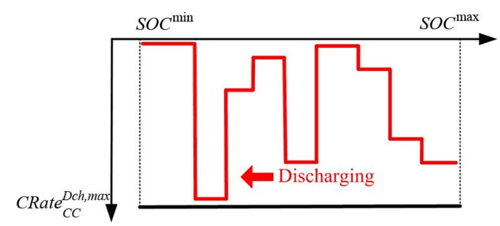

Fig. 5. Discharging scheduling for BSSs.

where $SOC_{CV,1}^{Ch}$, $SOC_{CV,2}^{Ch}$, and $SOC_{CV,3}^{Ch}$ are the transition SOCs of sub-stages 1, 2, and 3, respectively. $CRate_{CV,1}^{Ch}$, $CRate_{CV,2}^{Ch}$, and $CRate_{CV,3}^{Ch}$ are the charging currents of sub-stages 1, 2, and 3, respectively. Note that the transition SOC and charging current of each sub-stage can be determined from the CC-CV charging scheduling as illustrated in Fig. 1.

Therefore the whole charging procedure as shown in Fig. 3 including the CC stage, CV stage and floating stage can be expressed as

$$\begin{aligned}&\textbf{CC Stage}:\\&if\ SOC^{\min} < SOC(t) \le SOC_{CC}^{Ch}\\&CRate(t) = CRate_{CC}^{Ch} \quad (4a)\\&\textbf{CV Stage(3sub}-\textbf{stages)}:\\&\text{As formulated in Eq.(3)} \quad (4b)\\&\textbf{Floating Stage}:\\&if\ SOC_{CV,3}^{Ch} < SOC(t) \le SOC^{\max}\\&CRate(t) = CRate_{FL}^{Ch} \quad (4c)\end{aligned}$$

where $SOC^{\min}$ and $SOC^{\max}$ are the allowable minimum and maximum SOCs, respectively. For most batteries, $SOC^{\min}$ is 5% to 20% of the batteries' rated capacity and $SOC^{\max}$ can be 100% of the batteries' rated capacity. $CRate_{CC}^{Ch}$ and $CRate_{FL}^{Ch}$ are the charging currents of CC stage and floating stage, respectively.

The paper assumes that the existing battery management system (BMS) in BSS has been operating effectively; thus, the BMS functions including balancing charging/discharging and voltage/current/temperature monitoring are not included in the proposed BSS model. Besides, the battery terminal voltage recovery which affects the battery efficiency after a high charging/discharging rate is not included in this proposed model too. Since the battery's terminal voltage recovery is a transient behavior, it is more suitable to be analyzed by the model proposed in [21] and [22]. This paper tries to develop a steady-state mathematical model for BSSs; and therefore, the battery terminal voltage recovery is not discussed.

For simplicity, a single sub-stage CC charging for CV stage is used in the following derivations. In order to cope with the intermittent output of PVGSs, the charging/discharging scheduling of BSSs should be changed hourly at least. Fig. 4 illustrates a charging scheduling for BSSs with respect to the load variations and intermittent outputs of PVGSs. From Fig. 4, it can be seen that the charging current of each stage as illustrated in Fig. 3 will be changed to the allowable maximum charging current of each stage and be used to restrict the charging scheduling. In Fig. 4, $CRate_{CC}^{Ch,\max}$, $CRate_{CV}^{Ch,\max}$, and $CRate_{FL}^{Ch,\max}$ are the allowable maximum charging currents for CC, CV, and floating stages, respectively. Discharging scheduling is simpler and the procedure as illustrated in Fig. 5 is restricted by the allowable maximum discharging current ($CRate_{CC}^{Dch,\max}$) and $SOC^{\min}$.

Using the mathematical model as proposed in (2) and (4), and the charging/discharging scheduling as illustrated in Figs. 4 and 5, the $CRate$ (single sub-stage CC charging for CV stage used) allowed in the charging procedure can be expressed as

$$\begin{aligned}&\textbf{CC Stage}:\\&if\ SOC^{\min} \le SOC(t) \le SOC_{CC}^{Ch}\\&then\ 0 \le CRate(t) \le CRate_{CC}^{Ch,\max} \quad (5a)\\&\textbf{CV Stage (Single sub}-\textbf{stage)}:\\&if\ SOC_{CC}^{Ch} \le SOC(t) \le SOC_{CV}^{Ch}\\&then\ 0 \le CRate(t) \le CRate_{CV}^{Ch,\max} \quad (5b)\\&\textbf{Floating Stage}:\\&if\ SOC_{CV}^{Ch} \le SOC(t) \le SOC^{\max}\\&then\ 0 \le CRate(t) \le CRate_{FL}^{Ch,\max}. \quad (5c)\end{aligned}$$

The $CRate$ allowed in the discharging procedure is

$$\begin{aligned}&\textbf{Discharging}:\\&if\ SOC^{\min} \le SOC(t) \le SOC^{\max}\\&then\ 0 \le CRate(t) \le CRate_{CC}^{Dch,max}. \quad (5d)\end{aligned}$$

A practical and realistic mathematical model for BSSs has been proposed. The proposed model is suitable for power system analysis and can simulate the CC/CV charging, the discharging procedure and the SOC variation. The proposed model can be used for steady-state power system analysis such as spinning reserve, voltage regulation, peak load shifting, renewable energy integration, etc. However, only the renewable energy integration, especially line loss minimization for distribution systems interconnected with sizeable PVGSs, is formulated and implemented in this paper.

III. Optimal Charging/Discharging Scheduling

A. PVGS Output Calculation

PVGS has intermittent output characteristic associated with the random phenomenon of solar irradiance. References [28] and [29] revealed that Beta probability density function (pdf) can be used to model the solar irradiance effectively after a comparison of the different probability density distributions with the random phenomenon of solar irradiance. Therefore, the solar irradiance distribution can be written as [29]

$$f_b(s) = \begin{cases} \frac{\Gamma(\alpha+\beta)}{\Gamma(\alpha)\Gamma(\beta)} s^{(\alpha-1)}(1-s)^{(\beta-1)} & 0 \le s \le 1, \alpha, \beta \ge 0 \\ 0 & \text{otherwise} \end{cases} \tag{6a}$$

$$\beta = (1-\mu)\left(\frac{\mu(1-\mu)}{\sigma^2} - 1\right) \tag{6b}$$

$$\alpha = \frac{u\beta}{1-\mu} \tag{6c}$$

where $\Gamma(\bullet)$ is the gamma function, s is the random variable of solar irradiance $(\mathrm{kW/m^2})$, $f_b(S)$ is the Beta distribution function of s, α and β are the parameters of Beta distribution function, respectively, and μ and σ are the mean and standard deviation of s.

The output power of a PVGS is dependent on the solar irradiance and ambient temperature of the site as well as the parameters of the PV module used. The output power operating at maximum power point at solar irradiance s can be calculated by [28]

$$T_{cy} = T_A + s\left(\frac{N_{OT} - 20}{0.8}\right) \tag{7a}$$

$$I_y = s[I_{sc} + K_i(T_{cy} - 25)] \tag{7b}$$

$$V_y = V_{oc} - K_v^* T_{cy} \tag{7c}$$

$$FF = \frac{V_{MPPT} * I_{MPPT}}{V_{oc} * I_{sc}} \tag{7d}$$

$$P_o(s) = N^* FF^* V_y^* I_y \tag{7e}$$

where T_{cy} and T_A are the PV module temperature and ambient temperature, respectively. N_{OT}, I_{sc}, and V_{oc} are the nominal operating temperature, the short-circuit current, and the open-circuit voltage of PV module, respectively. K_v and K_i are the voltage temperature coefficient and current temperature coefficient, respectively. FF is the fill factor. N is the number of PV modules used in the PVGS. I_{MPPT} and V_{MPPT} are the current and voltage at maximum power point. P_o is the output power of PVGS at solar irradiance s.

Equation (7a) shows that the PV module temperature is a function of the nominal operating temperature, ambient temperature and solar irradiance. Equation (7b) shows that the PV output current is a function of the PV module temperature, short-circuit current, current temperature coefficient and solar irradiance. Equation (7c) illustrates that the PV output voltage is a function of the PV module temperature, open-circuit voltage and voltage temperature coefficient. If the PV parameters and operating conditions were measured or calculated, then the power output considering maximum power point can be obtained by (7d) and (7e). The expected output power at solar irradiance $s(EP(s))$ can be expressed as

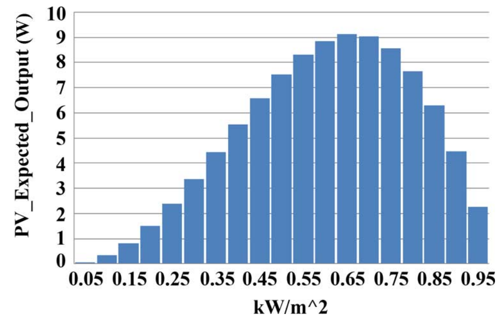

Fig. 6. Expected output power of the PV module.

$$EP(s) = P_o(s)^* f_b(s) \tag{8a}$$

and the expected total output power (ETP) at a specified time period can be calculated by

$$ETP = \int_0^1 P_o(s)^* f_b(s) ds. \tag{8b}$$

For example, if a PV module with the following parameters [30]: T_A : 30.76°C, N_{OT} : 43°C, I_{MPPT} : 7.76 A, V_{MPPT} : 28.36 V, I_{SC} : 8.38 A, V_{oc} : 36.96 V, K_i : 0.00545 A/°C and K_V : 0.1278 V/°C is used. The mean and standard derivation of solar irradiance at a specified time period is $0.525\ \mathrm{kW/m^2}$ and $0.212\ \mathrm{kW/m^2}$, respectively. The expected output power of the PV module with respect to solar irradiance can be calculated by (6)–(8) and the expected output powers with an interval $0.05\ \mathrm{kW/m^2}$ are illustrated in Fig. 6. The expected total output power obtained by summing the expected output powers in Fig. 6 is 97.179 W. Note that if the time period is one hour then the PV module is expected to output 97.179 Wh.

B. Problem Formulation

This paper aims to design an optimal charging/discharging scheduling of BSSs to minimize the line loss for distribution systems interconnected with sizeable PVGSs. One of the major advantages of BSS is its fast response time, which enables it to cope with the intermittent output of PVGSs effectively. The charging/discharging scheduling should be changed hourly at least with respect to the load variations and intermittent output of PVGSs. The objective function is to minimize the line loss and can be expressed as

$$\min \sum_{h=1}^{T} P_{Loss,h} \tag{9a}$$

where $P_{Loss,h}$ is the line loss for the distribution system at time period h. T is the analysis period.

Since the solar irradiance s is a random variable, the PVGSs' outputs and line loss will also be stochastic; therefore, the line loss can be formulated in the expected value and be rewritten as

$$\min E\left(\sum_{h=1}^{T} \sum_{l=1}^{lnum} I_{br,l,h}^2 R_{br,l}\right) \tag{9b}$$

where $E(\bullet)$ is the expected value function, *lnum* is the line number of distribution system, $R_{br,l}$ is the resistance of line l, and $I_{br,l,h}$ is the current of line l at time period h.

$I_{br,l,h}$ is a function of line parameters, loads, PVGSs' outputs and charging/discharging scheduling of BSSs, and can be written as

$$I_{br,l,h} = f(\mathbf{R}_{br}, \mathbf{X}_{br}, \mathbf{P}_{L,h}, \mathbf{Q}_{L,h}, \mathbf{P}_{PV,h}, \mathbf{P}_{BT,h}) \quad (10)$$

where $\mathbf{R}_{br}$ and $\mathbf{X}_{br}$ are vectors of line resistance and line reactance, respectively. $\mathbf{P}_{L,h}$, $\mathbf{Q}_{L,h}$, $\mathbf{P}_{PV,h}$ and $\mathbf{P}_{BT,h}$ are vectors of real power of load, reactive power of load, real power of PVGS and real power of BSS at time period h, respectively. Since the power factor of most inverters used for REGSs is close to 1.0, the reactive powers of PVGS and BSS are almost 0. Therefore, only the real powers for PVGS and BSS are considered in (10). Equation (10) can be solved by a load flow program.

The constraints for distribution systems, PVGSs and BSSs should be integrated into an optimization problem; and the equality and inequality constraints should at least include

$$P_{S,h} + \sum_{i=1}^{bnum} P_{L,i,h} + \sum_{i=1}^{pvnum} P_{PV,i,h} + \sum_{i=1}^{btnum} P_{BT,i,h} + P_{Loss,h} = 0 \quad (11a)$$

$$0 \le P_{PV,i,h} \le P_{PV,i}^{\max} \quad i = 1 \cdots pvnum \quad (11b)$$

$$0 \le \|P_{BT,i,h}\| \le P_{BT,i}^{\max} \quad i = 1 \cdots btnum \quad (11c)$$

$$SOC_i^{\min} \le SOC_{i,h} \le SOC_i^{\max} \quad i = 1 \cdots btnum \quad (11d)$$

$$V_i^{\min} \le V_{i,h} \le V_i^{\max} \quad i = 1 \cdots bnum \quad (11e)$$

$$0 \le \|I_{br,i,h}\| \le I_{br,i}^{\max} \quad i = 1 \cdots lnum \quad (11f)$$

where $P_{S,h}$, $P_{L,i,h}$, $P_{PV,i,h}$, and $P_{BT,i,h}$ are the real power of substation, real power of load bus i, real power of PVGS i, and charging or discharging power of BSS i at time period h, respectively. $bnum$, $pvnum$, and $btnum$ are the bus number of distribution system, the number of PVGS and the number of BSS, respectively. $P_{PV,i}^{\max}$ and $P_{BT,i}^{\max}$ are the allowable maximum output powers of PVGS and BSS, respectively. $SOC_{i,h}$ is the SOC of BSS i at time period h. $SOC_i^{\max}$ and $SOC_i^{\min}$ are the allowable maximum and minimum SOC of BSS i. $V_{i,h}$ is the voltage of bus i at time period h. $V_i^{\max}$ and $V_i^{\min}$ are the allowable maximum and minimum voltage of bus i. $I_{br,i,h}$ is the current of line i at time period h. $I_{br,i}^{\max}$ is the allowable maximum current of line i.

Equation (11a) is the power flow (11b) and (11c) are the output power constraint and charging or discharging power constraint for PVGS and BSS, respectively. Equation (11d) is the SOC constraint of BSS. Equations (11e) and (11f) are bus voltage and line current constraints for distribution systems, respectively. The expected output power of PVGS, the charging/discharging procedures of BSS and the SOC variation as formulated in (8), (5), and (2), respectively, need to be integrated into the solution procedure of the optimal charging and discharging scheduling of BSSs. The charging/discharging rates are considered as control variables and allowable maximum charging/discharging rates which can be acquired from BSS manufactures are considered as constraints. If the charging/discharging rates are within the maximum allowable charging/discharging rates recommended by the BSS manufactures, the effects of charging/discharging rates on the useful life and residual operation cycles of BSS can be greatly reduced. Therefore, the proposed scheduling will not degrade the safety and life of BSSs.

TABLE I
STRING ARRANGEMENTS AT TIME PERIOD H

String	*CRate (C)*	String	*CRate (C)*
00000	0	10000	0
00001	-0.025	10001	0.025
00010	-0.05	10010	0.05
00011	-0.075	10011	0.075
00100	-0.1	10100	0.1
00101	-0.125	10101	0.125
00110	-0.15	10110	0.15
00111	-0.175	10111	0.175
01000	-0.2	11000	0.2
01001	-0.225	11001	0.225
01010	-0.25	11010	0.25
01011	-0.05	11011	0.05
01100	-0.05	11100	0.05
01101	-0.025	11101	0.025
01110	-0.025	11110	0.025
01111	0	11111	0

C. Solution Technique

The optimization problem as formulated in (9)–(11) is a combinatorial constrained problem with a non-linear and non-differential objective function. The optimization formulations proposed in this paper can be solved by mixed integer programming (MIP) or artificial intelligence (AI) algorithms. This paper does not focus on the solution techniques of optimization; therefore, only a commonly-used GA-based algorithm [31], [32] is implemented to find the optimal solution. Main steps of the GA used in solving the proposed optimization problem can be summarized as follows:

1) Coding: representing the problem by bit strings. The possible charging and discharging powers of BSSs for the analysis period need to be formulated in each population. For example, if the allowable maximum charging and discharging power is set to be 0.25 C of a BSS. That is, for a BSS with rated capacity of 200 kWh, the maximum charging and discharging power is 50 kW. If the adjustable minimum charging and discharging power is 0.025 C, then a 5-bit string, with a total of 32 arrangements, can be used to model part of a population at time period h. Table I shows the string arrangements for different charging and discharging power at time period h. Since the allowable maximum charging and discharging power and adjustable minimum charging and discharging power are 0.25 C and 0.025 C, respectively, it means that only 21 arrangements are used for the 5-bit string. Other arrangements can be considered as invalid arrangements or used for other charging and discharging powers as shown in Table I. If the BSS is committed hourly, then a population will be composed of 120 bits.
2) Initialization: initializing the population. GA operates with a set of populations. The initial populations could be

seeded with heuristically chosen strings or at random. In our tests, all initial populations are randomly generated.

3) Evaluation: determining which population is better and deciding which ones to mate. The evaluation is a procedure to determine the fitness value of each population. The fitness value can be defined as the summation of objective function as formulated in (9b) and the penalty factors caused by the violations of constraints formulated in (11); therefore, the fitness value of the proposed optimal problem can be expressed as

$$\begin{aligned} fitness = E&\left(\sum_{h=1}^{T}\sum_{l=1}^{lnum} I_{br,l,h}^2 R_{br,l}\right) \\ &+ \sum_{h=1}^{T}\sum_{i=1}^{pvnum} PF_{PV,i,h} \\ &+ \sum_{h=1}^{T}\sum_{i=1}^{btnum} PF_{BT,i,h} \\ &+ \sum_{h=1}^{T}\sum_{i=1}^{btnum} PF_{SOC,i,h} \\ &+ \sum_{h=1}^{T}\sum_{i=1}^{bnum} PF_{V,i,h} \\ &+ \sum_{h=1}^{T}\sum_{i=1}^{lnum} PF_{IBR,i,h} \end{aligned} \tag{12a}$$

where $PF_{PV,i,h}$, $PF_{BT,i,h}$, $PF_{SOC,i,h}$, $PF_{V,i,h}$, $PF_{IBR,i,h}$ are the penalty factors for constraints of (11b) to (11f), respectively. For example, the can be defined as

$$\begin{aligned} &if\ SOC_i^{\min} \le SOC_{i,h} \le SOC_i^{\max} then \\ &PF_{SOC,i,h} = 0\ else\ PF_{SOC,i,h} = K_{SOC}. \end{aligned} \tag{12b}$$

The $SOC_{i,h}$ is estimated by (2), (3), and (5) in the solution procedure.

4) Crossover: exchanging information between two mates. Populations with lower fitness values should have a higher probability of generating offspring and are copied into the next generation.

5) Mutation: the process of randomly modifying the value of a string position with a small probability. It ensures that the probability of searching any region in the problem space is never zero and prevents complete loss of genetic material through mate and crossover.

The GA parameters used in the test cases are population size: 200, crossover rate: 0.5, mutation rate: 0.03, maximum iteration number: 300 and penalty factors: 10 000.

IV. Test Results and Discussions

The proposed method was implemented with Borland C++ on a Windows based PC. A distribution feeder acquired from Taiwan Power Company as shown in Fig. 7 is used in the following tests. The 24-hour real powers and reactive powers of loads for the typical summer and winter days are shown in Fig. 8. The power factors of the feeder can also be obtained

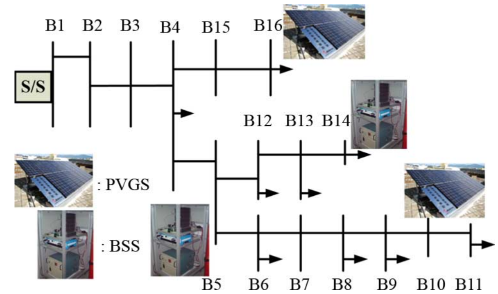

Fig. 7. A 16-bus test feeder.

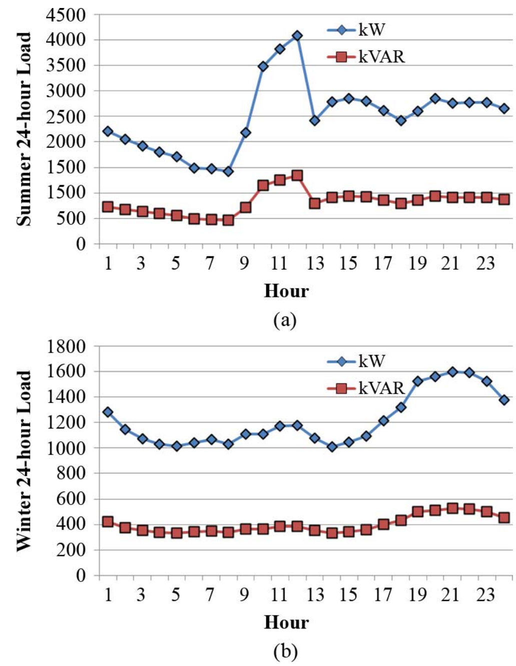

Fig. 8. 24-hour load profiles of the test feeder. (a) Summer. (b) Winter.

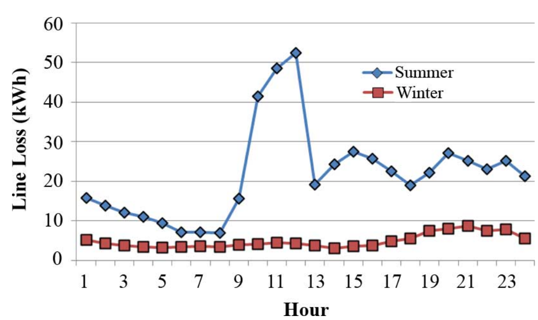

Fig. 9. 24-hour line losses.

from Fig. 8. The hourly line losses for the feeder before the installation of PVGSs and BSSs are shown in Fig. 9. The total line losses for the summer and winter days are 523.5 kWh and 117.3 kWh, respectively. The corresponding hourly solar irradiance for the summer and winter days acquired from Taiwan Weather Bureau are shown in Table II. The time step considered in this paper is 1 hour since the solar irradiance data acquired from Taiwan Weather Bureau is in an hourly basis. Smaller time steps can be used in this paper if more accurate solar irradiance data can be acquired.

TABLE II
SOLAR IRRADIANCES OF THE TEST FEEDER

	Summer (kW/m^2)		Winter (kW/m^2)	
Hour	Mean	Standard Deviation	Mean	Standard Deviation
6	0.007	0.021	0.000	0.000
7	0.081	0.036	0.001	0.006
8	0.237	0.056	0.067	0.042
9	0.400	0.087	0.205	0.082
10	0.523	0.127	0.337	0.120
11	0.632	0.156	0.443	0.142
12	0.663	0.162	0.516	0.161
13	0.657	0.164	0.539	0.158
14	0.612	0.147	0.479	0.151
15	0.497	0.143	0.378	0.124
16	0.349	0.116	0.241	0.085
17	0.203	0.081	0.087	0.061
18	0.068	0.063	0.002	0.008
19	0.003	0.012	0.000	0.000

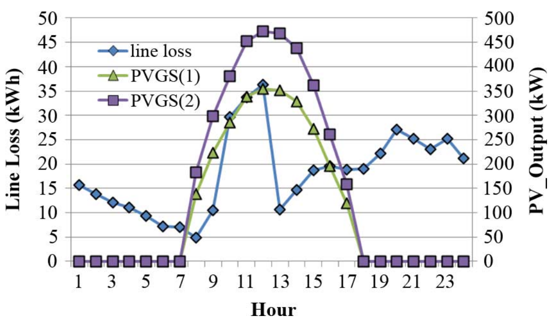

Fig. 10. PVGSs' outputs and line losses for the summer day.

For test purposes, two PVGSs and BSSs are installed in the test feeder of Fig. 7. The PV module used in the test cases is the same as this used in Section III. The PVGSs with 3000 and 4000 PV modules, which have 660 kW and 880 kW installed capacities, are installed at buses 10 and 16, respectively. After the installation of two PVGSs, the hourly expected output powers of PVGSs and the hourly expected line loss for the summer day are shown in Fig. 10. $\mathrm{PVGS}(1)$ and $\mathrm{PVGS}(2)$ refer to the PVGSs at buses 10 and 16, respectively. Note that only the results for the summer day are shown due to limited space. The expected total line losses for the summer and winter days are 437.0 kWh and 101.5 kWh, respectively.

Two BSSs with 3000 kWh and 4000 kWh installed capacities are installed at buses 5 and 14, respectively. The parameters for these two BSSs are as follows:

- Initial $SOCs$ for buses 5 and 14 are 0.33 and 0.5, respectively.
- $SOC^{\max}$ and $SOC^{\min}$ are 1.0 and 0.05, respectively.
- $CRate_{CC}^{Ch,\max}$ and $CRate_{FL}^{Ch,\max}$ are 0.25 C and 0.05 C, respectively.
- Two sub-stage CC charging process is used for CV stage and $CRate_{CV,1}^{Ch,\max}$ and $CRate_{CV,2}^{Ch,\max}$ are 0.15 C and 0.10 C, respectively
- $CRate_{CC}^{Dch,\max}$ is -0.25 C .
- SOC_{CC}^{Ch} is 0.6. $SOC_{CV,l}^{Ch}$ and $SOC_{CV,2}^{Ch}$ and $SOC_{CV,1}^{Ch}$ are 0.75 and 0.95, respectively.
- B^{Ch} and B^{Dch} are 0.95 and 0.95, respectively.
- The adjustable minimum charging and discharging power is $0.025\ C$.

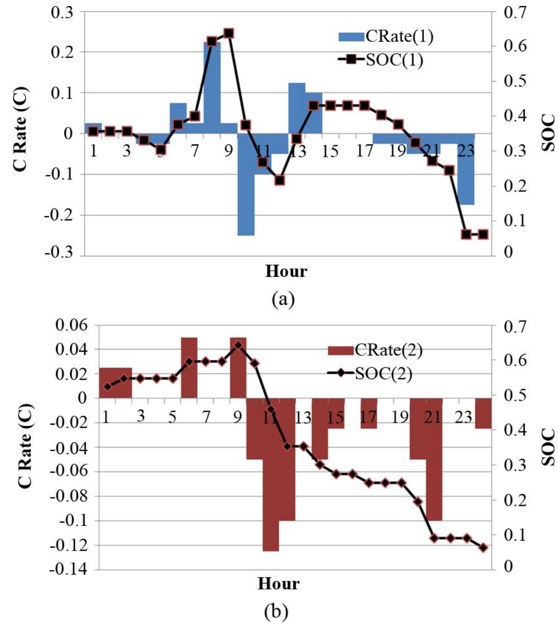

Fig. 11. Charging/discharging CRate and SOC for the summer day. (a) $\mathrm{BSS}(1)$. (b) $\mathrm{BSS}(2)$.

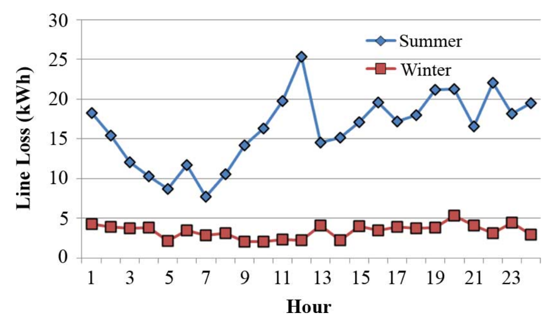

Fig. 12. 24-hour line losses for the optimal scheduling.

The charging and discharging scheduling is committed hourly and the analysis period is 24 hours. Using the formulas and solution technique as proposed in Section III to solve the optimization problem, the optimal charging/discharging of BSSs and the hourly line losses are shown in Figs. 11 and 12, respectively. $\mathrm{BSS}(1)$ and $\mathrm{BSS}(2)$ refer to the BSSs at buses 5 and 14, respectively. From Figs. 11 and 12, it can be seen that the BSSs with optimal charging/discharging scheduling are committed with the PVGSs to minimize the line loss. The expected total line losses in the summer and winter days can be reduced to 390.4 kWh and 81.5 kWh, respectively.

Fig. 13 shows the comparative hourly line losses without PVGS and BSS, with PVGS, as well as with PVGS and BSS for the test feeder in the summer and winter days, respectively. The total line losses without PVGS and BSS, with PVGS, and with PVGS and BSS in the summer day are 523.5 kWh, 437.0 kWh, and 390.4 kWh, respectively. The total line losses without PVGS and BSS, with PVGS and with PVGS and BSS in the winter day are and 117.3 kWh, 101.5, and 81.5 kWh, respectively. Note that if the BSSs do not commit with the PVGSs and is charged in the hours of off-peak load and discharged in

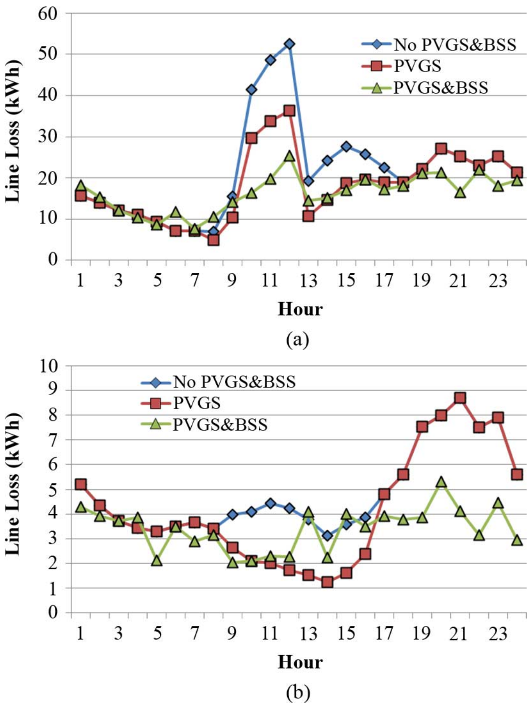

Fig. 13. Comparative 24-hour line losses. (a) Summer. (b) Winter.

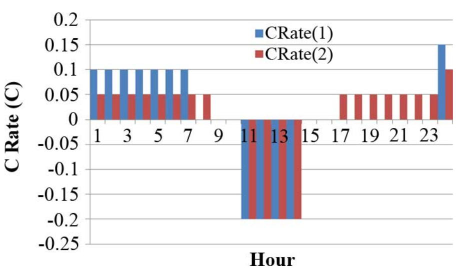

Fig. 14. Traditional charging/discharging scheduling.

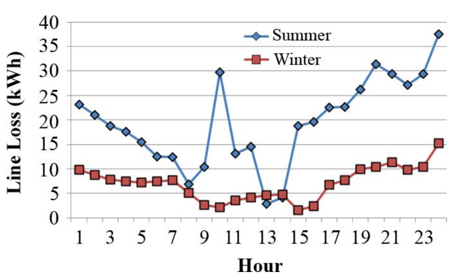

Fig. 15. 24-hour line losses for the traditional scheduling.

the hours of peak load, for example, the charging/discharging scheduling as illustrated in Fig. 14, then the expected total line losses for the summer and winter days are 467.4 kWh and 169.0 kWh, respectively. The hourly line losses for the test feeder in the summer and winter days operated in the traditional charging/discharging scheduling are illustrated in Fig. 15. It can be seen that if the BSSs cannot commit effectively with PVGSs then BSSs may increase line loss and degrade the operation performance. Therefore, from the test results, it can be seen that the proposed optimal scheduling has improved the operation performance.

Different parameters and installed capacities of PVGSs and BSSs, which can be changed for different application purposes and operation requirements, will result in different results. For example, if the allowable minimum SOCs are changed to 0.15, then the total line losses are 400.7 kWh and 86.4 kWh for the summer and winter days, respectively. Besides, more constraints for BSS can also be added to (11) for operation requirements. For example, if the end SOCs of a day must be restricted, the following constraints can be added:

$$SOC_{i,24} \leq SOC_i^{end} \quad i = 1 \cdots btnum \tag{13}$$

where $SOC_{i,24}$ and SOC_i^{end} represent the end SOC and allowable end SOC of a day for BSS i, respectively.

If SOC_i^{end} is 0.3, then the total line losses are 415.3 kWh and 91.8 kWh for the summer and winter days, respectively. Although different test results are obtained, the proposed formulas and solution technique do not need major modifications. The GA parameters might also affect the test results; however, the effects are not significant in the test cases. An hourly basis analysis may not be appropriate, especially, if the BSSs are designed to react on the fluctuating power injections of REGS or sudden outage events. However, if more accurate solar irradiance data can be acquired then a more accurate solution based on the proposed method can be obtained accordingly.

V. Conclusions

This paper proposed a mathematical model for BSSs and used the minimum line loss problem to verify the performance of the proposed BSS model. Test results showed that if the commitment between PVGSs and BSSs can be determined effectively, then the advantages of BSSs can be achieved. Since the proposed BSS model and charging/discharging scheduling can be demonstrated, the proposed method has great potentials to be used in the analysis of other BSS applications such as regulation service, voltage support, peak-load shifting, and reliability improvement. Those issues will be discussed in the future works.

References

[1] Engineering Guide for Integration of Distributed Generation and Storage into Power Distribution Systems, EPRI Tech. Rep. TR-100419, 2000.
[2] A. Woyte, V. V. Thong, R. Belmans, and J. Nijs, "Voltage fluctuations on distribution level introduced by photovoltaic systems," *IEEE Trans. Energy Convers.*, vol. 21, no. 1, pp. 202–209, Mar. 2006.
[3] P. Denholma and R. M. Margolis, "Evaluating the limits of solar photovoltaics next term (PV) in traditional electric power systems," *Energy Policy*, vol. 35, pp. 2852–2861, 2007.
[4] W.-H. E. Liu, "Analytics and information integration for smart grid applications," in *Proc. IEEE Power and Energy Soc. General Meeting*, 2010, pp. 1–3.
[5] A. Vojdani, "Smart integration," *IEEE Power and Energy Mag.*, vol. 6, no. 6, pp. 71–79, Nov.-Dec. 2008.
[6] A. S. Bouhouras, G. T. Andreou, D. P. Labridis, and A. G. Bakirtzis, "Selective automation upgrade in distribution networks towards a smarter grid," *IEEE Trans. Smart Grid*, vol. 1, no. 3, pp. 278–285, 2010.
[7] S. E. Collier, "Ten steps to a smarter grid," *IEEE Ind. Applicat. Mag.*, vol. 16, no. 2, pp. 62–68, 2010.
[8] R. W. Uluski, "The role of advanced distribution automation in the smart grid," in *Proc. IEEE Power and Energy Soc. General Meeting*, 2010, pp. 1–5.
[9] Electric Energy Storage Systems, Cigre Working Group C5.15, 2011.

[10] M. Kintner-Meyer, M. Elizondo, P. Balducci, V. Viswanathan, C. Jin, X. Guo, T. Nguyen, and F. Tuffner, Energy Storage for Power Systems Applications: A Regional Assessment for the Northwest Power Pool (NWPP), U.S. Department of Energy, Apr. 2010.
[11] W. Steeley, Functional Requirements for Electric Energy Storage Applications on the Power System Grid, EPRI Tech. Rep. 1022544, 2011.
[12] D. Rastler, Electricity Energy Storage Technology Options: A White Paper Primer on Applications, Costs, and Benefits, EPRI Tech. Rep. 1020676, 2010.
[13] I. Hadipaschalis, A. Poullikkas, and V. Efthimiou, "Overview of current and future energy storage technologies for electric power applications," *Renew. Sustain. Energy Rev.*, vol. 13, no. 6/7, pp. 1513–1522, Aug./Sep. 2009.
[14] P. Denholma and R. M. Margolis, "Evaluating the limits of solar photovoltaics (PV) in electric power systems utilizing energy storage and other enabling technologies," *Energy Policy*, vol. 35, pp. 4424–4433, 2007.
[15] M. Perrin, Y. M. Saint-Drenan, F. Mattera, and P. Malbranche, "Lead acid batteries in stationary applications: Competitors and new markets for large penetration of renewable energies," *J. Power Sources*, vol. 144, pp. 402–410, 2005.
[16] H. Kanchev, L. Di, F. Colas, V. Lazarov, and B. Francois, "Energy management and operational planning of a microgrid with a PV-based active generator for smart grid applications," *IEEE Trans. Ind. Electron.*, vol. 58, no. 10, pp. 4583–4592, 2011.
[17] L. Bo and M. Shahidehpour, "Short-term scheduling of battery in a grid-connected PV/battery system," *IEEE Trans. Power Syst.*, vol. 20, no. 2, pp. 1053–1061, May 2005.
[18] S. Teleke, M. E. Baran, S. Bhattacharya, and A. Q. Huang, "Rule-based control of battery energy storage for dispatching intermittent renewable sources," *IEEE Trans. Sustain. Energy*, vol. 1, no. 3, pp. 117–124, 2010.
[19] Y. Riffonneau, S. Bacha, F. Barruel, and S. Ploix, "Optimal power flow management for grid connected PV systems with batteries," *IEEE Trans. Sustain. Energy*, vol. 2, no. 3, pp. 309–320, 2011.
[20] Y.-H. Liu, J.-H. Teng, and Y.-C. Lin, "Search for an optimal rapid charging pattern for lithium ion batteries using ant colony system algorithm," *IEEE Trans. Ind. Electron.*, vol. 52, no. 5, pp. 1328–1336, Oct. 2005.
[21] V. H. Johnson, "Battery Performance Models in ADVISOR," *J. Power Sources*, pp. 321–329, 2002.
[22] H. J. Valerie, D. Z. Matthew, and A. P. Ahmad, "Development and validation of a temperature-dependent resistance/capacitance battery model for ADVISOR," in *Proc. Electric Vehicle Symp.*, Oct. 20–24, 2000.
[23] S. Abu-Sharkh and D. Doerffel, "Rapid test and non-linear model characterization of solid-state lithium-ion batteries," *J. Power Sources*, pp. 266–274, 2004.
[24] S.-W. Luan, J.-H. Teng, D.-J. Lee, Y.-Q. Huang, and C.-L. Sung, "Charging/discharging monitoring and simulation platform for li-ion batteries," in *Proc. IEEE TENCON*, , Nov. 2011.
[25] M. Coleman, C. K. Lee, C. Zhu, and W. G. Hurley, "State-of-Charge determination from emf voltage estimation: Using impedance, terminal voltage and current for lead-acid and llithium-ion batteries," *IEEE Trans. Ind. Electron.*, vol. 54, no. 5, pp. 2550–2557, Oct. 2007.
[26] Y. S. Lee, W. Y. Wang, and T. Y. Kuo, "Soft computing for battery state-of-Charge (BSOC) estimation in battery string systems," *IEEE Trans. Ind. Electron.*, vol. 55, no. 1, pp. 229–239, Jan. 2008.
[27] I. S. Kim, "Nonlinear state of charge estimator for hybrid electric vehicle battery," *IEEE Trans. Power Electron.*, vol. 23, no. 4, pp. 2027–2034, Jul. 2008.
[28] Y. M. Atwa, E. F. El-Saadany, M. M. A. Salama, and R. Seethapathy, "Optimal renewable resources mix for distribution system energy loss minimization," *IEEE Trans. Power Syst.*, vol. 25, no. 1, pp. 360–370, Feb. 2010.
[29] Z. M. Salameh, B. S. Borowy, and A. R. A. Amin, "Photovoltaic module-site matching based on the capacity factors," *IEEE Trans. Energy Convers.*, vol. 10, no. 2, pp. 326–332, Jun. 1995.
[30] 220 W PV Module, Solar Gate Technology Corporation, Feb. 2012. [Online]. Available: http://www.solargatetech.com.
[31] D. E. Goldberg*, Genetic Algorithms: Search, Optimization and Machine Learning*. Reading, MA: Addison-Wesley, 1989.
[32] J.-H. Teng and C.-N. Lu, "Optimum fault current limiter placement with search space reduction technique," *IET Gen., Transm., Distrib.*, vol. 4, no. 4, pp. 485–494, 2010.

Jen-Hao Teng (SM'11) received the B.S., M.S., and Ph.D. degrees in electrical engineering from the National Sun Yat-Sen University, Kaohsiung, Taiwan, in 1991, 1993, and 1996, respectively.

He was with I-Shou University, Kaohsiung, Taiwan, from 1998 to 2010. He has been with National Sun Yat-Sen University since 2011. His current research interests are smart grid, advanced distribution automation, design and analysis of green and renewable energy, utilization of heuristic techniques in power system, RFID and ZigBee applications, etc.

Shang-Wen Luan received the B.S. and M.S. degrees in electrical engineering from the I-Shou University, Kaohsiung, Taiwan, in 2004 and 2008, respectively. He is pursuing the Ph.D. degree in electrical engineering of the I-Shou University.

His current research interests include distribution automation, smart grid, and application of RFID, ZigBee, and smart meter in power systems.

Dong-Jing Lee was born in Kaohsiung County, Taiwan, on December 19, 1979. He received the M.S. and Ph.D. degrees from the Department of Electrical Engineering, National Chung Kung University, Tainan, Taiwan, in 2004 and 2008, respectively.

He has been with the Industrial Technology Research Institute since 2008. His interests are power system dynamics and fuel cells.

Yong-Qing Huang was born in 1978 in Taoyuan, Taiwan. He received the M.S. degree in electrical engineering from the National Taiwan University of Science and Technology in 1995.

His current research interests are MicroGrid control, power system stability and renewable energy, etc.